Elastomers

All-Elastomeric, Strain-Responsive Thermochromic Color Indicators

Cunjiang Yu, Yihui Zhang, Dongkai Cheng, Xuetong Li, Yonggang Huang, and John A. Rogers**

Recent advances in materials for stretchable electronics create new areas of application, particularly in systems that involve intimate integration with the human body. Examples include wearable electronics,[1–6] soft surgical instruments,[5,7–13] and skin-integrated health/wellness monitors.[1,14–18] Many envisioned systems require schemes for visual information display. Such functionality can be provided by organic or inorganic light emitting diodes (LEDs), either as arrays of non-stretchable devices joined by deformable interconnects,[7,19,20] or as elements in buckled geometries.[19,21] Intrinsically stretchable LEDs have also recently been achieved, using all polymer designs.[22] Here we present a simple, non-emissive option in display materials that likewise offer intrinsic stretchability. The approach uses elastomeric composites of thermochromic materials and metallic particles as the photonic and electronic components, respectively, in concepts that build on related materials[23] for flexible displays. We show, additionally, that the types of stretchable displays introduced here can be used as colorimetric indicators of mechanical strain.

Dr. C. Yu,[+] D. Cheng
Department of Materials Science and Engineering
Frederick Seitz Materials Research Laboratory
University of Illinois at Urbana-Champaign
Urbana, IL, 61801, USA
Dr. Y. Zhang,[+] Dr. X. Li
Department of Civil and Environmental Engineering
and Department of Mechanical Engineering
Northwestern University
Evanston, IL, 60208, USA
Dr. Y. Zhang
Center for Mechanics and Materials
Tsinghua University
Beijing, 100084, China
Dr. X. Li
College of Mechanical Engineering
Yanshan University
Qinhuangdao, 066004, China
Prof. Y. Huang
Department of Civil and Environmental Engineering
Department of Mechanical Engineering
Center for Engineering and Health
and Skin Disease Research Center
Northwestern University
Evanston, IL, 60208, USA
E-mail: y-huang@northwestern.edu
Prof. J. A. Rogers
Department of Materials Science and Engineering
Chemistry, Mechanical Science and Engineering
Electrical and Computer Engineering
Beckman Institute for Advanced Science and Technology
and Frederick Seitz Materials
Research Laboratory
University of Illinois at Urbana-Champaign
Urbana, IL, 61801, USA
E-mail: jrogers@illinois.edu

[+]These authors contributed equally to this work.

DOI: 10.1002/smll.201302646

The thermochromic elastomer uses a well-mixed dispersion of leuco dye (black 47C, LCR Hallcrest) contained in microcapsules and embedded in a silicone elastomer matrix (Smooth-on Inc.), in a construction that is similar to previous reports.[23] (See the Experimental Section). The dye uses a fluoran chemistry, with the reversible ability to open (colored) and close (colorless) lactone rings in the presence of acids.[24,25] The microencapsules contain mixtures of leuco dye with a color developer and a low melting point solvent. At low temperature, the developer and leuco dye form a complex that favors the colored ring-open state. Upon heating, the solvent melts, and the developer and dye dissociate. The leuco dye then favors the colorless, ring-closed state. Such transformations occur in a reversible manner.[23–26] For the case explored here, at temperatures below ≈47 °C the dye is black; at higher temperatures, the mismatch between the index of refraction of the microencapsulated dye and the surrounding silicone matrix leads to strong optical scattering and a white appearance. The net effect, then, is a temperature activated, reversible switching between black and white. **Figure 1**a,b presents confocal and scanning electron microscope images of this type of composite. At room temperature, the composite is black. As the temperature rises above 47 °C, the color changes to bright white, as illustrated by reflectance measurements across the visible range (Figure 1c). Mechanical stretching (e.g., deformation to strains of 30%, 60%, etc.) leads to minimal change in the color, as is also indicated in Figure 1c.

Patterns of stretchable conductors integrated directly with this type of thermochromic elastomer provide spatially controlled Joule heating for localized/selectable color switching. Here, we exploit a silver (Ag) particle filler in a silicone matrix, similar to previous reports.[27,28] Details appear in the Experimental Section. Figure 1d presents an SEM image of such a conductive elastomer with 80 wt% Ag. The conductivity increases monotonically with Ag loading, as

NANO MICRO small

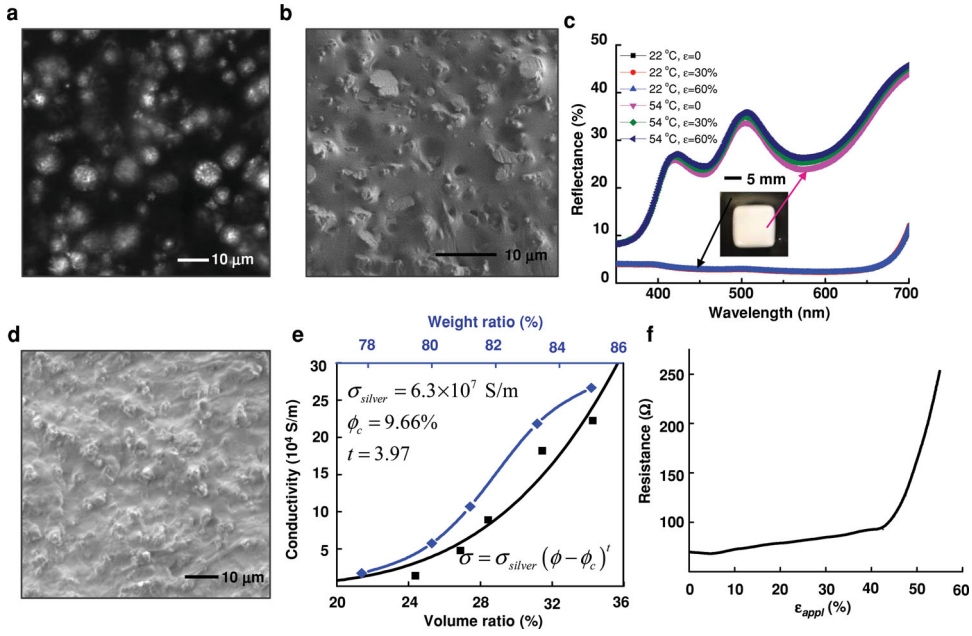

Figure 1. Characterization of materials for stretchable displays/indicators and colorimetric strain sensors. (a) Confocal microscope image of a thermochromic elastomer composites. The encapsulated leuco dye appear white. (b) SEM image of the thermochromic elastomer. (c) Optical reflectance from a 100 μm thick sheet of thermochromic elastomer, measured at low (22 °C, inactivated) and high (54 °C, activated) temperature and at different levels of stretching (0%, 30%, 60%). (d) SEM image of a conductive elastomer. (e) Electrical conductivity of conductive elastomers with different mixing ratios of Ag filler. The blue dots correspond to the conductivities at different weight ratios, and the blue fitting curve reveals the trend of monotonically increase. The black dots correspond to the conductivities at different volume ratios, and the black fitting curve shows power-law percolation relation of such elastomer. (f) Resistance as a function of applied strain (ε_{appl}) for a conductive elastomer wire.

shown by the blue curve in Figure 1e. The functional dependence shows a power-law relationship, consistent with percolation theory[29]: $\sigma = \sigma_{silver}(\phi - \phi_C)^t$, as seen by the black curve in Figure 1e, where ϕ_C is the critical volume fraction, i.e. the percolation threshold, and t is the exponent related to the formation of continuous clusters through the composite above the critical volume fraction. Other conductive stretchable composites, such as those that use fillers of carbon black,[30,31] carbon nanotubes (CNTs),[16,30,32] etc., can also be considered. Elastomers with conductivity in the range of ≈10^4–10^5 S/m are well matched to the requirements of the application considered here.

Replica molding techniques enable such conductive elastomers to be patterned into geometries with feature sizes from the micron to centimeter range. Here, composite pastes of Ag and uncured PDMS fill into trenches defined by patterns of photoresist, similar to processes described previously.[30,33,34] Measurements of electrical resistance of a patterned conductive trace (30 mm × 150 μm × 50 μm) embedded in an insulating elastomer under uniaxial stretching appear in Figure 1f. The results indicate that the resistance increases gradually (30%) up to elongations of ≈40%, and then much more rapidly for additional stretching. These behaviors, which result from a combination of compressive forces associated with the Poisson effect and increases in separation between Ag particles,[35] provide a range of responses that are useful in both stretchable information display and visual strain indicators, as described next. Improved stretching characteristics can be obtained using different formulations and materials, as described elsewhere.[35–38]

Figure 2a illustrates the procedures for fabricating a complete system on a thin polyimide film (Kapton NH, DuPont, 75 μm), as a temporary support for the processing. Casting a layer of the conductive elastomer prepolymer into trenches defined in a thick layer of photoresist, followed by thermal curing defines the heater elements and interconnects. Spin casting and curing a uniform layer (100 μm) of thermochromic elastomer prepolymer completes the fabrication. Peeling the entire system away from the photoresist and polyimide substrate, as shown in Supporting Information Figure S1 (right), yields an isolated elastomer sheet, capable of electrically programmable color change. A ribbon cable and printed circuit board (PCB) serve as interfaces for measurement and testing, as shown in Figure S1.

Various display geometries and indicator layouts can be realized in this simple scheme. A 3 × 3 array of heaters connected in series provides an example. Control of the widths and configurations of the conductive traces defines the spatial distribution of Joule heating. For the case of Figure 2b, the regions of traces designed to provide heating have widths of 150 μm; others regions have widths of 500 μm. Switchback structures (7 repeats, with 500 μm spacing to cover an area of 4.1 mm × 4.5 mm) define heating areas, corresponding to individual pixel elements. The resistance of each heater is ≈84 Ω. The device can accommodate a full range of deformation, including non-uniform stretching and twisting, as illustrated in Figure 2c, consistent with its elastomeric character. Applying a bias of 4 V across two of the pixels (top left and top right) selectively changes their color from black to white within ≈1 s, as illustrated in Figure 2d. The corresponding power consumption is ≈55 mW.

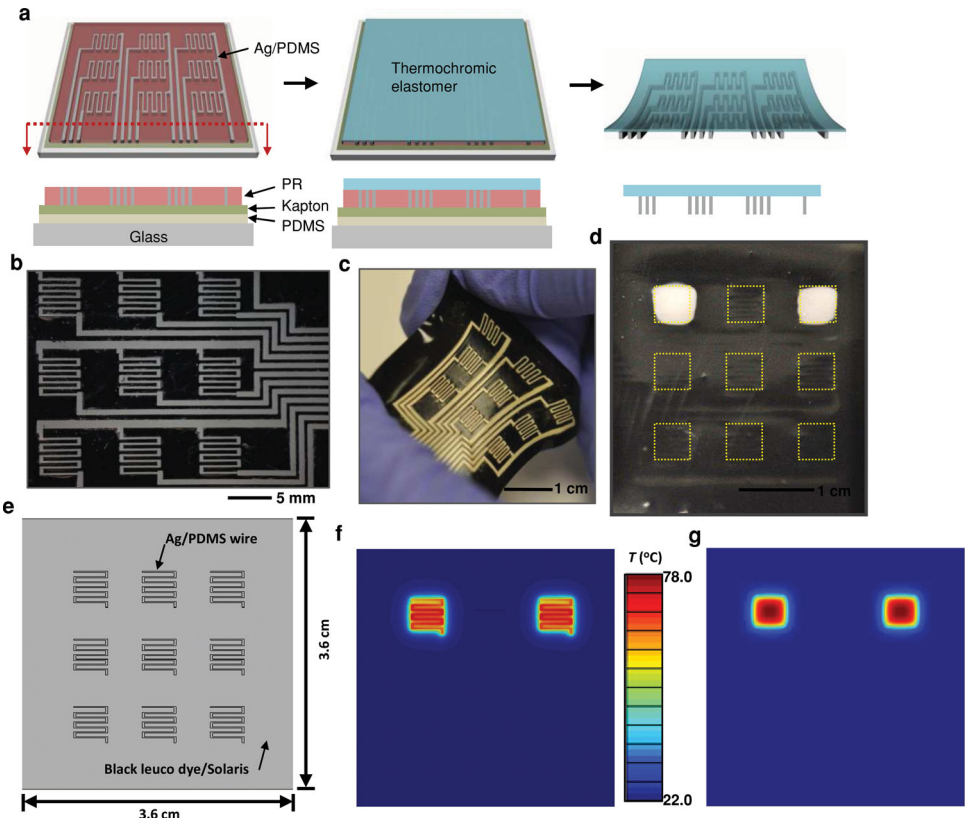

Figure 2. (a) Schematic major steps for fabricating the all-elastomer thermochromic indicator. (b) Optical image of an elastomeric display/indicator that includes a 3 × 3 array of heaters defined by switchbacks in the conductive traces. (c) Optical image of the device under non-uniform stretching. (d) An elastomeric display/indicator, viewed from the front during activation of the top corner pixels. (e) Geometry for finite element model of the device. (f) Full 3D FEA and (g) analytical results of the temperature distribution of the device during operation as in (d).

Finite element analysis (FEA) (see the Supporting Information for details) establishes aspects of heat flow that determine the power efficiency and response time, as well as considerations in materials and device layouts that define these characteristics. Figure 2e presents a schematic illustration of the three-dimensional (3D) computational model. Figure 2f shows the temperature at the top surface of the substrate for the case of 55 mW applied to each of the two pixels at the top right and top left. Analytical models (See SI for details) of heat conduction reveal the mechanisms of heat confinement and provide guidelines to enable effective control of individual pixels. Figure 2g shows the temperature distribution defined by analytical solution (Equation (S6)), consistent with full 3D FEA results, that indicate effective heat confinement at the pixel location. The analytic model predicts that a minimum power for color switching of ≈48 mW, which agrees reasonably well with FEA result (≈50 mW) and experiment (≈55 mW). The solution (Equation (S6) in the Supporting Information) also reveals that the temperature distribution becomes more localized with an increase of the combined parameter, $hA/(k_{substrate}H_{substrate})$, as shown in Figure S2b, where $k_{substrate}$ and $H_{substrate}$ are the thermal conductivity and thickness of substrate, A is the area of heat source, and h is the heat transfer coefficient for natural convection with air. In other words, heat confinement can be improved by decreasing the thermal conductivity or thickness of the thermochromic elastomer, or by increasing the convection coefficient.

Another important performance parameter is the response time, which can be estimated by $L^2_{characteristic}/(\alpha_{substrate})$,[39] where $\alpha_{substrate}$ is the thermal diffusivity of the substrate and $L_{characteristic} = (w_{conducting\_wire} + s_{conducting\_wire})/2$ is the characteristic size of the switchback structure, and $w_{conducting\_wire}$ and $s_{conducting\_wire}$ represent the width and spacing of the conducting wire, respectively. For the experimental design parameters, the response time is calculated to be ≈1.03 s for the 3 × 3 array of heaters, which is comparable to experimental observation and is satisfactory for many envisioned applications. The time can be reduced by modifying the layout, such as the width of the heaters and space between them.

Figure 3a shows that the elastomer indicator with 3 × 3 pixel array in an undeformed state (top), and unixially stretched to strains of 20% (middle) and 40% (bottom). 3D FEA (see SI for details) that includes the detailed geometry of the system captures the mechanics. The computed deformation at 40% strain (Figure 3b), for example, agrees well with experimental images (Figure 3a). Since the modulus of the conductive traces is similar to that of the substrate, the strain transfers almost entirely, as shown in Figure S3. For 40% stretching, the maximum principal strain of the conducting polymer is ≈33%, which is far below the regime of strain (≈60%) that induces significant increases in resistivity. This result is consistent with the experimental observations in Figure 3a. The strain distribution (Figure 3c) in the

small NANO MICRO

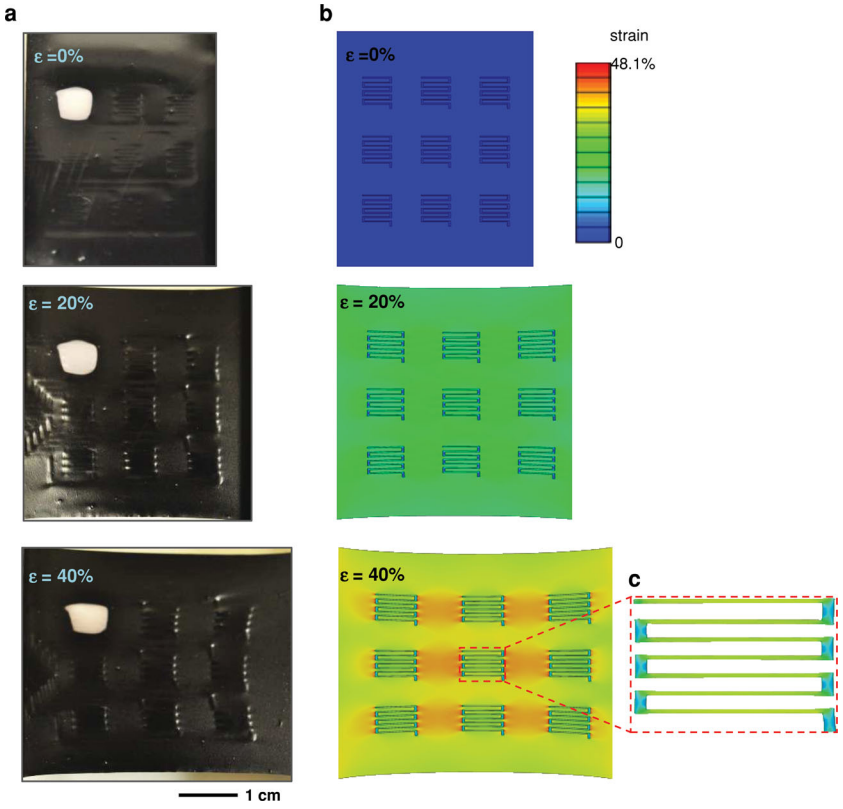

Figure 3. (a) Elastomeric display/indicator under different levels of stretching: unstretched (top), 20% (middle), and 40% (bottom). (b) Computed deformation and distribution of maximum principal strain under 40% stretching along horizontal direction. (c) Distribution of maximum principal strain in the conductive wire at the center pixel.

conducting wire is spatially uniform along the horizontally aligned segments.

By properly configuring the device layout and materials formulations, it is possible to exploit changes in the resistance of the conductive elastomer (Figure 1f) with strain to allow use as a visual indicator of strain. A device that demonstrates this possibility uses a zigzag shaped conductive trace in a sparse configuration, as in Figure S4. The overall resistance is 120 Ω. The left panel of **Figure 4**a shows an image of the indicator upon application of 3.5 V. As the the elastomer is stretched by 20% and then 50%, the pattern of the color changes, as demonstrated in the middle and right image of Figure 4a. In particular, the zigzag white line (left image of Figure 4a) transforms into a collection of isolated white segments along the horizontal direction (middle and right image of Figure 4a). Such changes arise from strain induced increases in resistance, and therefore extent of local heating. 3D FEA, as shown in Figure 4b, reveals the effects. For 50% stretching, the longitudinal strain in the horizontal conductive wires is ≈43% (shown in Table S1 and Figure S5), while that in the vertical wires is –17%, i.e. compression. This result is consistent with invariant volume during deformation, i.e., 43% elongation in the longitudinal direction induces 16.4% compression in the other two directions. The series connection of the horizontal and vertical wire segments ensures that the current is uniform throughout. The local heating power, therefore, is directly proportional to the local resistance: Joule heating increases along the horizontal wires, and diminishes along at the vertical wires, with increased tensile stretching. For regions adjacent to the vertical wires, where the original color is white, the color changes to black as the temperature is reduced below the threshold (≈47 °C). This capability suggests opportunities in colorimetric strain mapping, or strain induced color switching, in ways that might offer useful diagnostic function not easily obtained using other approaches.

In summary, thermochromic elastomers can be combined with conductive elastomers and elastomer substrates/encapsulants to yield a fully stretchable display and visual strain indicator. Experimental and theoretical investigations illustrate the key materials and mechanics aspects. This type of system could be integrated with other functional materials, to provide bioelectrical sensing and measurement capabilities, with potential for broad utility in biointegrated

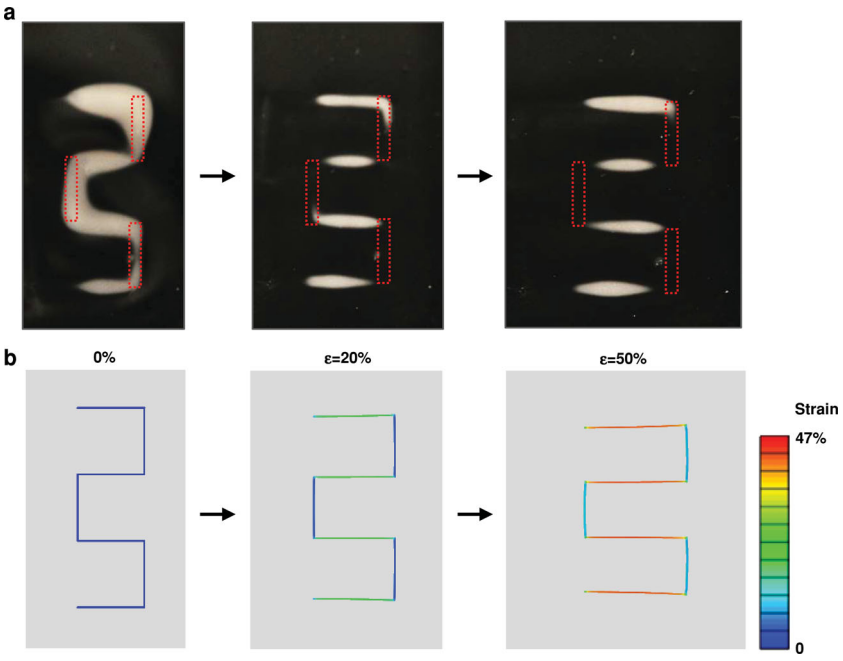

Figure 4. (a) Color transformation associated with heating by a zigzag wire, under different levels of stretching: unstretched (left), 20% (middle), and 50% (right). (b) Deformation and distribution of maximum principal strain corresponding to (a).

systems, where the elastomeric mechanics can be critically important.

Experimental Section

Preparing the Thermochromic Elastomer: The thermochromic elastomer uses mixtures of leuco dye (black, activation temperature = 47 °C) with a precursor to a silicone material (Solaris, Smooth-on Inc, weight ratio of part A:B = 1:1) at a weight ratio of 1:10. Spin-casting and thermally curing the resulting material at 110 °C yields thin films.

Preparing the Conductive Elastomer: The conductive elastomer uses mixtures of Ag particles (average diameter 2–3.5 μm, Sigma Aldrich) with a precursor to poly(dimethylsiloxane) (Sylgard 184, Dow Corning Inc., weight ratio of base:curing agent = 30:1) at different weight ratios, such as 4:1, 5:1, etc. A drill miller (DR260B, Black & Decker) was used for mixing. Heating at 80 °C for 2 h transforms the precursor into a solid form.

Characterizing the Thermochromic Elastomer: The modulus of the thermochromic elastomer was measured under uniaxial tensile loading with a dynamic mechanical analyzer (DMA) (TA Instruments, Q 800). The samples consisted of strips, 4 cm long, 5 mm wide, and 100 μm thick. The strips were tested by clamping the two ends and applying stepwise increased tensile force. A tensile modulus of 0.409 MPa was obtained from the slope of the linear part of the stress-strain curve. The results were based on the average of six individual samples.

The optical reflectance of the thermochromic elastomer at different temperatures was measured using a spectrometer (Cary 5G UV-VIS-NIR). A portable commercial thermoelectric heater/cooler (InbS1–031.021, WATRONIX, Inc.) was utilized to control the sample temperature. A thermocouple (Fluke 233, Fluke Corporation) was used to measure the temperature.

Characterizing the Conductive Elastomer: The modulus of the conductive elastomer was measured in the same way as the thermochromic elastomer. The tensile modulus was 0.893 MPa for conductive elastomer with 80 wt% Ag.

The electrical resistance was characterized by measurements on long, narrow wires (3 cm long, 150 μm wide and 50 μm thick) with contact pads (5 mm long, 1 mm wide and 50 μm thick) at their ends. The wires were supported by a Solaris or thermochromic elastomer substrate. The pads clamped to custom made cables (Figure S1) and a mechanical stretching apparatus. A multimeter (Fluke 233, Fluke Corporation) was used to measure the electrical resistance through an interfacing PCB.

Supporting Information

Supporting Information is available from the Wiley Online Library or from the author.

Acknowledgements

This work was supported by Office of Naval Research (N00014–10–1–0989). YH acknowledges the support from NSF (DMR-1242240 and CMMI-0749028) and the support from NSFC.

[1] X. Huang, W. H. Yeo, Y. H. Liu, J. A. Rogers, *Biointerphases* **2012**, *7*, 52.
[2] M. Ying, A. P. Bonifas, N. S. Lu, Y. W. Su, R. Li, H. Y. Cheng, A. Ameen, Y. G. Huang, J. A. Rogers, *Nanotechnology* **2012**, *23*, 344004.
[3] T. Sekitani, T. Someya, *MRS Bull.* **2012**, *37*, 236.
[4] M. Ramuz, B. C. K. Tee, J. B. H. Tok, Z. N. Bao, *Adv. Mater.* **2012**, *24*, 3223.
[5] D. P. J. Cotton, I. M. Graz, S. P. Lacour, *IEEE Sens. J.* **2009**, *9*, 2008.
[6] T. Vervust, G. Buyle, F. Bossuyt, J. Vanfleteren, *J. Textile Inst.* **2012**, *103*, 1127.
[7] D. H. Kim, N. S. Lu, R. Ghaffari, Y. S. Kim, S. P. Lee, L. Z. Xu, J. A. Wu, R. H. Kim, J. Z. Song, Z. J. Liu, J. Viventi, B. de Graff, B. Elolampi, M. Mansour, M. J. Slepian, S. Hwang, J. D. Moss, S. M. Won, Y. G. Huang, B. Litt, J. A. Rogers, *Nat. Mater.* **2011**, *10*, 316.
[8] D. H. Kim, J. Viventi, J. J. Amsden, J. L. Xiao, L. Vigeland, Y. S. Kim, J. A. Blanco, B. Panilaitis, E. S. Frechette, D. Contreras, D. L. Kaplan, F. G. Omenetto, Y. G. Huang, K. C. Hwang, M. R. Zakin, B. Litt, J. A. Rogers, *Nat. Mater.* **2010**, *9*, 511.
[9] D. H. Kim, S. D. Wang, H. Keum, R. Ghaffari, Y. S. Kim, H. Tao, B. Panilaitis, M. Li, Z. Kang, F. Omenetto, Y. G. Huang, J. A. Rogers, *Small* **2012**, *8*, 3263.
[10] J. Viventi, D. H. Kim, J. D. Moss, Y. S. Kim, J. A. Blanco, N. Annetta, A. Hicks, J. L. Xiao, Y. G. Huang, D. J. Callans, J. A. Rogers, B. Litt, *Sci. Transl. Med.* **2010**, *2*, 24ra22.
[11] O. Graudejus, B. Morrison, C. Goletiani, Z. Yu, S. Wagner, *Adv. Funct. Mater.* **2012**, *22*, 640.
[12] Z. Yu, O. Gaudejus, S. Lacour, S. Wagner, B. Morrison, *J. Neurotrauma* **2011**, *28*, A33.
[13] Z. Yu, O. Graudejus, C. Tsay, S. P. Lacour, S. Wagner, B. Morrison, *J. Neurotrauma* **2009**, *26*, 1135.
[14] W. H. Yeo, Y. S. Kim, J. Lee, A. Ameen, L. K. Shi, M. Li, S. D. Wang, R. Ma, S. H. Jin, Z. Kang, Y. G. Huang, J. A. Rogers, *Adv. Mater.* **2013**, *25*, 2773.
[15] D. H. Kim, N. S. Lu, R. Ma, Y. S. Kim, R. H. Kim, S. D. Wang, J. Wu, S. M. Won, H. Tao, A. Islam, K. J. Yu, T. I. Kim, R. Chowdhury, M. Ying, L. Z. Xu, M. Li, H. J. Chung, H. Keum, M. McCormick, P. Liu, Y. W. Zhang, F. G. Omenetto, Y. G. Huang, T. Coleman, J. A. Rogers, *Science* **2011**, *333*, 838.
[16] H. C. Jung, J. H. Moon, D. H. Baek, J. H. Lee, Y. Y. Choi, J. S. Hong, S. H. Lee, *IEEE Trans. Biomed. Eng.* **2012**, *59*, 1472.
[17] G. Schwartz, B. C.-K. Tee, J. Mei, A. L. Appleton, D. H. Kim, H. Wang, Z. Bao, *Nat. Comm.* **2013**, DOI: 10.1038/ncomms2832.
[18] M. Kaltenbrunner, T. Sekitani, J. Reeder, T. Yokota, K. Kuribara, T. Tokuhara, M. Drack, R. Schwödiauer, I. Graz, S. Bauer-Gogonea, S. Bauer, T. Someya, *Nature* **2013**, *499*,458.
[19] S. I. Park, Y. J. Xiong, R. H. Kim, P. Elvikis, M. Meitl, D. H. Kim, J. Wu, J. Yoon, C. J. Yu, Z. J. Liu, Y. G. Huang, K. Hwang, P. Ferreira, X. L. Li, K. Choquette, J. A. Rogers, *Science* **2009**, *325*, 977.
[20] T. Sekitani, H. Nakajima, H. Maeda, T. Fukushima, T. Aida, K. Hata, T. Someya, *Nat. Mater.* **2009**, *8*, 494.
[21] M. S. White, M. Kaltenbrunner, E. D. Głowacki, K. Gutnichenko, G. Kettlgruber, I. Graz, S. Aazou, C. Ulbricht, D. A. M. Egbe, M. C. Miron, Z. Major, M. C. Scharber, T. Sekitani, T. Someya, S. Bauer, S. Sariciftci, *Nat. Photonics* **2013**, *7*, 811.
[22] Z. B. Yu, X. F. Niu, Z. T. Liu, Q. B. Pei, *Adv. Mater.* **2011**, *23*, 3989.
[23] L. Y. Liu, S. L. Peng, W. J. Wen, P. Sheng, *Appl. Phy. Lett.* **2007**, *90*, 213508.
[24] T. Horiguchi, Y. Koshiba, Y. Ueda, C. Origuchi, K. Tsutsui, *Thin Solid Films* **2008**, *516*, 2591.
[25] Y. Hatano *Chemistry and Applications of Leuco Dyes* (ed: R. Muthyala) Plenum Press, New York, **2002**.
[26] A. C. Siegel, S. T. Phillips, B. J. Wiley, G. M. Whitesides, *Lab Chip* **2009**, *9*, 2775.

[27] T. Araki, M. Nogi, K. Suganuma, M. Kogure, O. Kirihara, *IEEE Electron Device Lett.* **2011**, *32*, 1424.
[28] Z. Li, R. W. Zhang, K. S. Moon, Y. Liu, K. Hansen, T. R. Le, C. P. Wong, *Adv. Funct. Mater.* **2013**, *23*, 1459.
[29] M. Niklaus, H. R. Shea, *Acta Mater.* **2011**, *59*, 830.
[30] N. Lu, C. Lu, S. Yang, J. Rogers, *Adv. Funct. Mater.* **2012**, *22*, 4044.
[31] A. R. Aiyar, C. Song, S. H. Kim, M. G. Allen, *Smart Mater. Struct.* **2009**, *18*, 115002.
[32] M. Knite, K. Ozols, J. Zavickis, V. Tupureina, I. Klemenoks, R. Orlovs, *J. Nanosci. Nanotechnol.* **2009**, *9*, 3587.
[33] M. J. Kim, J. Yoon, S. I. Park, J. A. Rogers, *Appl. Phys. Lett.* **2009**, *95*, 214101.
[34] K. S. Ryu, X. F. Wang, K. Shaikh, C. Liu, *J. Microelectromech. Syst.* **2004**, *13*, 568.
[35] K. Y. Chun, Y. Oh, J. Rho, J. H. Ahn, Y. J. Kim, H. R. Choi, S. Baik, *Nat. Nanotechnol.* **2010**, *5*, 853.
[36] M. K. Shin, J. Oh, M. Lima, M. E. Kozlov, S. J. Kim, R. H. Baughman, *Adv. Mater.* **2010**, *22*, 2663.
[37] L. Lin, S. Y. Liu, Q. Zhang, X. Y. Li, M. Z. Ji, H. Deng, Q. Fu, *ACS Appl. Mater. Inter.* **2013**, *5*, 5815.
[38] T. Sekitani, Y. Noguchi, K. Hata, T. Fukushima, T. Aida, T. Someya, *Science* **2008**, *321*, 1468.
[39] Y. H. Li, Y. Shi, J. Z. Song, C. F. Lu, T. I. Kim, J. A. Rogers, Y. G. Huang, *J. Appl. Phys.* **2013**, *113*, 144505.

Received: August 14, 2013
Revised: September 30, 2013
Published online: November 27, 2013